

Time-reversal and super-resolving phase measurements

K. J. Resch¹, K. L. Pregnell^{1,2}, R. Prevedel¹, A. Gilchrist^{1,2}, G. J. Pryde^{1,2}, J. L. O'Brien^{1,2} and A. G. White^{1,2}

¹Department of Physics ²Centre for Quantum Computer Technology University of Queensland, Brisbane QLD 4072, Australia

We demonstrate phase super-resolution can be obtained even in the absence of entangled states, allowing a significant reduction in experimental complexity. The key insight is to use the inherent time-reversal symmetry of quantum mechanics: we *measure*, as opposed to prepare, an entangled state and demonstrate phase super-resolution with 3, 4, and 6 photons. Our six-photon experiment demonstrates the highest phase super-resolution yet reported.

Common wisdom holds that entangled states are a necessary resource for many protocols in quantum information, ranging across quantum communication, quantum computation and quantum metrology. Quantum metrology promises super-precise measurement, where the precisions possible with classical states of light and matter are surpassed using quantum states [1]. In the last 20 years quantum metrology schemes have been proposed for improved optical [2, 3, 4, 5, 6, 7] and matter-wave [8] interferometry, atomic spectroscopy [9], and lithography [10, 11, 12]. The entangled states in these schemes give rise to *phase super-resolution*, where the interference oscillation occurs over a phase N-times smaller than one cycle of classical light [13, 14] and *phase super-sensitivity*, a reduction of phase uncertainty.

Many quantum metrology schemes are based on path-entangled number states. The canonical example is the NOON state [1], a two-mode state with either N photons in one mode and 0 in the other or vice-versa, i.e., $(|N\rangle|0\rangle + |0\rangle|N\rangle)/\sqrt{2}$. A deterministic optical source of path-entangled states is yet to be realised, as it requires optical nonlinearities many orders of magnitude larger than those possible with current technology. However, entangled states can be made *non-deterministically* using single-photon sources, linear optics, and photon-resolving detectors [15]. Applying this insight led to a flurry of proposals for non-deterministic generation of optical path-entangled states [16, 17, 18, 19]. While phase super-resolution with two-photons has been demonstrated often since 1990 [20, 21, 22, 23], phase super-resolution was demonstrated experimentally for 3-photon [13] and 4-photon [14] states only last year. As efficient photon sources and photon-number resolving detectors do not yet exist, all demonstrations to date necessarily used multiphoton coincidence post-selection, e.g. post-selecting the two-mode state[13], $(|3,0\rangle + |0,3\rangle)/\sqrt{2}$, or four-mode state[14], $(|2,2,0,0\rangle + |0,0,2,2\rangle)/\sqrt{2}$. Previous proposals for path-entanglement relied on the production of a large number of single photons, their non-deterministic combination into an entangled number-state, and photon-number resolving detection. Problematically, current photon sources are extremely dim and true photon-number resolving detectors are expensive and uncommon [24]. Our technique eliminates the need for exotic photon sources and detectors: we use a standard laser, photon counters, and multiphoton coincidence.

Figure 1a) depicts a method for probabilistically gen-

erating NOON states via linear optics and post-selection. Single photon states are prepared in each of the N input modes, $|\Psi_i\rangle = |11\dots1\rangle_{12\dots N}$, of a linear optical multiport interferometer[25], U_{multi} . The multiport can be of the symmetric variety, where every input mode is converted into an equal superposition of N output modes [16], or of an asymmetric variety, where not every input satisfies this condition [17]. With probability η , no photons are found in modes 3 through N and the state in modes 1 and 2 is the NOON state $(|N0\rangle_{12} + |0N\rangle_{12})/\sqrt{2}$. Any object that introduces a phase shift, ϕ , between modes 1 & 2 will introduce a relative phase shift of $N\phi$ between the two terms in the superposition—the factor of N gives rise to phase super-resolution. Maximum fringe visibility will be achieved when the system is measured in a state $\langle\psi_N|$ which has equal overlap, $\kappa_N = |\langle\psi_N|N0\rangle|^2 = |\langle\psi_N|0N\rangle|^2$, with both components of the NOON state. The probability of detecting a final state $\langle\Psi_f| = \langle\psi_N|_{12}\langle 0\dots0|_{3\dots N}$ after propagating through the multiport and phase shifter is $P = |\langle\Psi_f|U_\phi U_{\text{multi}}|\Psi_i\rangle|^2 = \eta\kappa_N(1 + \cos N\phi)$. This probability exhibits phase super-resolution since the fringes complete N oscillations over a single cycle of 2π .

Probabilities in quantum mechanics are invariant under time reversal [26, 27, 28], i.e., if we swap the input and measured states and suitably time-reverse the operation of the multiport, as shown in Figure 1b), the probability is unchanged, $P = |\langle\Psi_i|U_{\text{multi}}^\dagger U_\phi^\dagger|\Psi_f\rangle|^2 = \eta\kappa_N(1 + \cos N\phi)$. Time-reversing the process turns the difficult generation of N single photons into straightforward detection of N photons in coincidence, and turns the problematic detection of the vacuum into vacuum inputs which are automatically available with perfect fidelity. Finally, instead of measuring $\langle\psi_N|$, which typically requires complicated detection set-ups as shown in Figure 1, one can input a state $|\psi_N\rangle$ which is much simpler to generate, e.g., two equal amplitude coherent states which are easily obtained with a laser. This is nondeterministic measurement, as opposed to creation, of a NOON state.

This time-reversal technique is a simple example of a more general measurement technique introduced by Pregnell and Pegg [28, 29], where a linear optical device can be constructed which non-deterministically measures *any* target state, given *any* input state.

In our experiments the two equal amplitude coherent states are the vertical and horizontal polarisation modes of the one spatial mode, and we apply a phase shift, ϕ , between these modes. In classical interferometry, this will

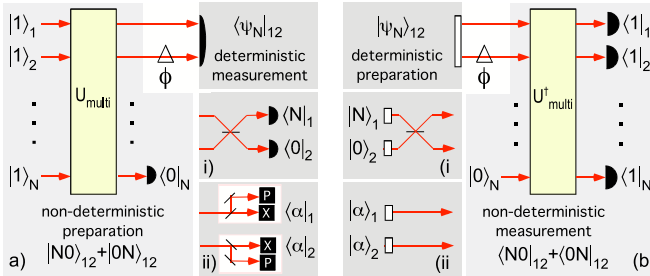


FIG. 1: Non-deterministic a) preparation & b) measurement of NOON states for phase super-resolution measurements.

a) *non-deterministic preparation*. Single photons are input in modes 1 to N of a multiport: heralded production of the NOON state occurs with efficiency, η , signalled by detection of no photons in modes 3 to N . A phase shift, ϕ , is induced between the output modes 1 & 2, which are sent to a *deterministic measurement* device that measures the state $|\psi_N\rangle$ that has equal overlap, κ_N , with both components of the NOON state. Examples include: i) a 50% beamsplitter that combines the two modes, so as to remove which path information, followed by two photon-number resolving detectors which measure $|N\rangle_1$ & $|0\rangle_2$, yielding[16] $\kappa_N^i=1/2^N$; ii) two coherent state detectors (each consisting of a 50% beamsplitter and two homodyne detectors to measure the amplitude and phase quadratures) that measure $|\alpha\rangle_1$ & $|\alpha\rangle_2$, yielding $\kappa_N^{ii}=\kappa_N^i/\sqrt{2\pi N}$ in the optimum case $|\alpha|^2=N/2$.
b) *deterministic preparation* of a state $|\psi_N\rangle$ that has equal overlap, κ_N , with both components of the NOON state. Examples include: i) a 50% beamsplitter that combines modes with N and 0 photons, $|N\rangle_1$ & $|0\rangle_2$, yielding $\kappa_N^i=1/2^N$; ii) two coherent states, $|\alpha\rangle_1$ & $|\alpha\rangle_2$, yielding $\kappa_N^{ii}=\kappa_N^i/\sqrt{2\pi N}$ in the optimum case $|\alpha|^2=N/2$. A phase shift, ϕ , is induced between the modes 1 & 2 and then input to a *non-deterministic measurement* device that consists of a multiport with vacuum inputs into modes 3 to N . Heralded detection of a NOON state occurs with efficiency, η , signalled by detection of a single photon in output modes 1 to N of the multiport.

yield one oscillation for $0 < \phi < 2\pi$. Figure 2a) shows the ideal symmetric multiport interferometer for $N=3$, Figure 2b) our experimental realisation with an intrinsically-stable interferometer. The symmetric multiport is set up with an internal phase, β , such that each input mode is transformed to an equal superposition of the three output modes. The three-fold coincidence count rates as a function of the phase, ϕ , are shown in Figure 2c), with three distinct oscillations within a single phase cycle. This is in contrast to the fringes observed in the singles rates, Figure 2d), which undergo only a single oscillation over the same range. This is the experimental signature of phase super-resolution. We emphasize that this was achieved without *production* of a path-entangled state, which would have had the signature of a flat singles rates over an optical cycle [14, 23].

This phase super-resolution can be understood by realising that the coincidence rate is determined entirely by the product of the singles rates, as must be the case in the absence of higher-order interference phenomena. An $N \times N$ multiport can be set up such that the detection probability in the k^{th} output mode is $P_k \propto 1 + \cos(\phi + 2\pi k/N + \varphi)$,

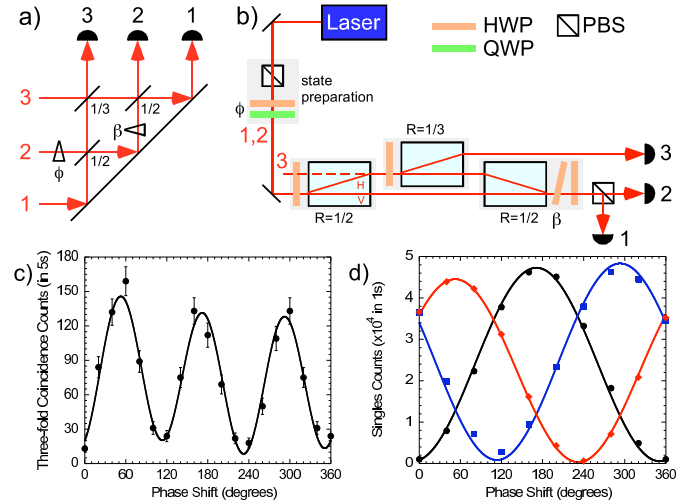


FIG. 2: a) Ideal symmetric 3×3 multiport, U_{multi} , constructed from 2×2 beamsplitters with reflectivities as shown. Each input mode transforms to an equal superposition of the three output modes if the internal phase, β , is properly set. Here, we input no light (vacuum) into mode 3 and coherent states in modes 1 & 2, with a phase shift ϕ , applied between them. b) Schematic of our experimental 3×3 multiport. The light source was an horizontally-polarised attenuated 12 mW He:Ne laser. We make the vertical & horizontal modes the same amplitude and introduce the phase shift using a half-wave plate (HWP) followed by a quarter-wave plate at an angle of 45°. Changing the angle of the HWP by $\phi/4$ changes the relative phase between the coherent states by ϕ . The multiport is constructed of beamsplitters comprised of a polarising beam displacers and HWPs: two of the HWPs in the interferometer are set at 22.5° forming effective 1/2 beamsplitters with the beam displacers, a third is set at 17.6° so that 2/3 of the light intensity takes the upper path. The tilted HWP is set at 0° to the optic axis and sets the internal phase, β . The output modes are sent to three single-mode fibre-coupled single photon counting detectors D1–D3. The singles rate is the number of photons per second detected by an individual detector: in this experiment the maximum was 5×10^4 Hz. The three singles rates are recorded individually, the three-fold coincidence rate is measured using two ORTEC 567 Time-to-Amplitude Converter/Single Channel Analyzer (TAC/SCA) modules each with a 1.5μs coincidence window. In practice, due to a restricted number of recording channels, the singles were measured immediately after a coincidence run. To avoid saturation effects in our detectors, the mean number of photons per coincidence window must be one or less: here, this was at most 0.07. c) 3-fold coincidence rate as a function of phase, ϕ , exhibiting three distinct oscillations within a single phase cycle. The main source of uncertainty is Poissonian statistics: error bars represent the square root of the count rate. The solid line is a fit, reduced $\chi^2=1.6$, to a product of 3 sinusoidal fringes, as explained in the text. d) Singles rates as a function of ϕ for detectors D1(black), D2(blue), and D3(red), each exhibiting only one oscillation per phase cycle. Error bars are contained within the data points; the solid lines are the individual sinusoidal fringes obtained above, scaled by a constant factor that matches the amplitude to the data but does not alter the visibility or phase of each fringe. In the ideal case the phase differences between these adjacent singles fringes would be $2\pi/3$; our fit procedure gives 122° & 119°.

where φ is a constant phase offset. The N -fold coincidence probability is then simply the product of the single mode probabilities, i.e., $P_{1\dots N} \propto 1 + \cos(N\phi + \Delta_0)$ which clearly exhibits N oscillations per cycle. The phase offset, Δ_0 is a function of N and φ .

To show that the N -fold coincidence rate can indeed be explained as a product of the singles fringes, the three-fold coincidence fringe pattern was fit to a product of 3 sinusoidal fringes, $c_i + c_i v_i \sin(\phi + \delta_i)$ where v_i is the visibility, and c_i & δ_i are amplitude and phase offsets of the i^{th} fringe. The resulting fit – the solid line in Figure 2c) – is very good, with a reduced χ^2 of 1.6. The solid lines in Figure 2d) are the 3 sinusoidal fringes obtained above, scaled by a constant factor that matches the amplitude to the data but does not alter the visibility or phase of each fringe. Again the agreement is very good.

It is clear that production of path-entangled states is not required for phase super-resolution: it suffices that the measurement system have non-zero overlap, κ_N , with a NOON state. Our experiment could be further simplified by replacing the photon counters with intensity detectors and the multiphoton coincidence with electronic multiplication of the signals. (The time reversed version of this corresponds to a quite exotic input state, and is of little practical interest). Practically, this can only be done with photon fluxes much higher than we consider here, to lift the signal above the electronic noise floor of the square-law detectors. This is inadvisable if the phase shift being measured is significantly affected by high photon flux, e.g., biological specimens or a mirror reacting to radiation pressure.

Scaling up symmetric multiports to $N > 3$ can be done with a polynomial number of nested standard interferometers [25] which would be arduous to phase lock, or a single $N \times N$ fused fibre except that it is not known how to control the large set of internal phases [16]. However, a symmetric multiport is not required for phase super-resolution: for even- N , an asymmetric multiport can be constructed as shown in Figures 3 a) and b). Figures 3 c) and d) show the coincidence data for $N=4$ and $N=6$, clearly exhibiting 4 and 6 oscillations per cycle, respectively. Again, the singles rates from each detector, shown in Figures 3 e) and f), exhibit only one oscillation over the same range. The latter case is the largest phase super-resolution reported to date. We apply the same fitting procedure as previously, now with 4 and 6 sinusoidal fringes, yielding the solid line fits shown. The fits are good and very good, with reduced χ^2 of 6 and 1.7 respectively. We believe that the high value for χ^2 in the $N=4$ case is due to observed amplitude instability of the signal at D3 during the course of the coincidence measurement. Note that the coincidence fringes for all three experiments differ from a pure sinusoid, due to small variations in the visibilities, amplitudes, and phases of the underlying singles rates. These differences become more pronounced for larger values of N .

Experiments using nonclassical light have demonstrated phase super-resolution for three-photon [13] and

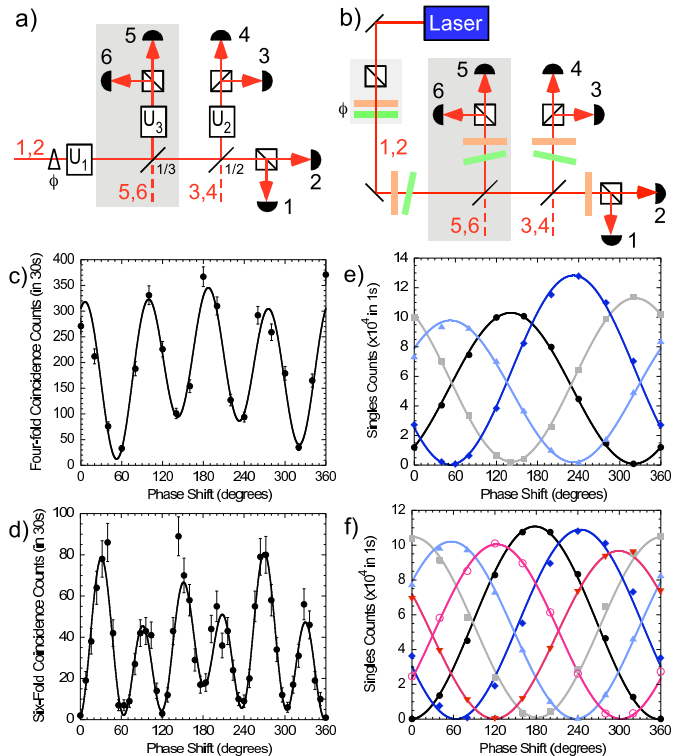


FIG. 3: a) Ideal asymmetric 4×4 (6×6) multiport constructed from 2×2 beamsplitters with reflectivities as shown. Modes 1 & 2 are populated with orthogonally-polarised coherent states in the same spatial mode and a phase shift, ϕ , is applied between them. Vacuum is input in modes 3 & 4 (and 5 & 6). Polarisation rotations, U_1 , U_2 (and U_3) were used to set the phase of the singles fringe pattern so that one detector reached an interference minimum every 22.5° of phase cycle, ϕ , for $N=4$ (every 15° for $N=6$). Polarising beamsplitters split the output modes into their orthogonal polarisation components which are detected by single photon counters: phase super-resolution will be seen in the 4-fold (6-fold) coincidences. b) Experimental schematic of our asymmetric 4×4 (6×6) multiport. The light source and phase shift, ϕ , were applied as before. The multiport was constructed using a pellicle for $N=4$ (plus an uncoated microscope slide for $N=6$). Beam splitter reflectivities were not ideal, we equalised the rates with lossy coupling (the slide angle of incidence was $\sim 10^\circ$ to avoid polarisation effects). Polarisation rotations are realised using a combination of waveplates as shown: the orientation and tilt of each waveplate was adjusted so as to give the desired phase shift. The maximum singles rate was 1.3×10^5 Hz: coincidence counting was performed using up to 3 TAC/SCAs and an ORTEC CO4020 Quad Logic Unit. For $N=4$ all pulse length inputs to the Quad were set to $1.5\mu\text{s}$ as were the coincidence windows on the TAC/SCA (for $N=6$, $5\mu\text{s}$). At most, the mean number of detected photons per coincidence window was 0.15 and 0.48 for the $N=4$ and $N=6$ cases respectively. c) & d) 4-fold & 6-fold coincidence rates as a function of ϕ respectively exhibiting four and six distinct oscillations within a single phase cycle. The main source of uncertainty is Poissonian statistics: error bars are calculated by taking the square root of the count rate. The solid lines are fits, reduced $\chi^2=6$ and 1.6, respectively, to a product of 4 and 6 sinusoidal fringes, as described in the text. e) & f) Singles rates as a function of ϕ for detectors D1(black), D2(grey), D3(blue), D4(cyan), D5(red), and D6(pink), each exhibiting only one oscillation per phase cycle. Error bars are contained within the data points; the solid lines are the individual sinusoidal fringes obtained and scaled as in Fig. 2d). In the ideal case the phase differences between these adjacent singles fringes would be $2\pi/N$; our fit procedure gives differences for $N=4$ of 92° , 90° and 90° ; and for $N=6$ of 55° , 66° , 56° , 62°

four-photon states [14]. Such nonclassical light sources are notoriously dim and as such the signal coincidence rates for three-fold and four-fold cases were limited to 5 Hz [13] and 0.1 Hz [14] respectively. In a state-of-the-art multiphoton entanglement experiment involving five-photon coincidence, but not phase super-resolution, the rate was limited to 175 counts in 2 hours [30], or about 0.024 Hz. Since we can use a laser, which is not nearly so limited in brightness, we were able to achieve phase super-resolution in a *six*-photon coincidence rate of about 2.7 Hz, which is several orders of magnitude better than rates from current nonclassical light sources. Furthermore, owing to the high-visibility singles and extremely stable construction of the multiports, our fringe patterns all enjoyed high visibility. Fitting a simple sinusoidal pattern, and without any background subtraction, the fringe visibilities for the $N=3$, $N=4$ and $N=6$ cases are respectively $81\pm3\%$, $76\pm2\%$, and $90\pm2\%$ —well exceeding the raw visibilities of $42\pm3\%$ and $\sim61\%$ for the previous 3-photon [13] and 4-photon [14] phase super-resolution measurements.

Let us comment briefly on phase super-sensitivity. Classical states of light can estimate phase shifts to within $\Delta\phi \propto 1/\sqrt{N}$, where \bar{N} is the mean number of photons passing the phase shifter [1]. If NOON states could be prepared deterministically, or in the non-deterministic case, if production success could be heralded before the state passed through the phase shifter, then the phase sensitivity would be $\Delta\phi \propto 1/N$, where N is the number of photons passing the phase shifter—a sub-shot noise measurement. Note that if the photons are produced by unheralded spontaneous parametric down-conversion, any advantage beyond just using the pump beam in a

classical interferometer is immediately lost due to the low intrinsic conversion efficiency, typically 10^{-6} – 10^{-10} . Even if single photons were available efficiently, no unheralded nondeterministic scheme considered to date, be it preparation or measurement, can provide phase super-sensitivity for large N because the exponentially small probability of success[16, 17, 18, 19], η , far outweighs the square-root advantage.

We have demonstrated high-visibility phase super-resolution, a feature of many quantum metrology schemes, using a scheme that in principle non-deterministically *measures*, as opposed to non-deterministically produces, path-entangled states. The advantage of our method is that it greatly simplifies experimental requirements, in particular allowing the use of standard laser sources, yielding high count rates and correspondingly reduced uncertainties. In a six-photon experiment, we have shown phase super-resolution of up to 6 oscillations per cycle by encoding our coherent states in polarisation and measuring a polarisation-dependent phase shift. This improvement in phase resolution is homologous to that achievable with a standard path interferometer driven at a wavelength of 105.5 nm—one-sixth the wavelength of our He:Ne laser. Inverting the roles of state production and measurement is an application of a more general time-reversal analysis technique [28, 29]: given the dramatic improvement demonstrated here, it remains an interesting open question as to which other quantum technologies will benefit from this technique.

This work was supported by the Australian Research Council. We wish to thank Timothy Ralph and Gerard Milburn for discussions, and Howard Wiseman, David Pegg and Paul Meredith for helpful comments on the manuscript. RP's present address is Institut für Experimentalphysik, Universität Wien, Vienna, Austria. Submitted 30 August, 2005.

[1] H. Lee, P. Kok, P. & J. P. Dowling, *Proc. Sixth Int. Conf. on Quant. Commun., Meas. and Comp.* (eds Shapiro, J. H. & Hirota, O.) 223-229 (Rinton Press, Princeton, 2002).
[2] B. Yurke, *Phys. Rev. Lett.* **56**, 1515-1517 (1986).
[3] M. Hillery, & L. Mlodinow, *Phys. Rev. A* **48**, 1548-1558 (1993).
[4] M. J. Holland, & K. Burnett, *Phys. Rev. Lett.* **71**, 1355-1358 (1993).
[5] C. Brif, & A. Mann, *Phys. Rev. A* **54**, 4505-4518 (1996).
[6] Z. Y. Ou, *Phys. Rev. A* **55**, 2598-2609 (1997).
[7] R. A. Campos, C. C. Gerry, & A. Benmoussa, *Phys. Rev. A* **68**, 023810 (2003).
[8] J. P. Dowling, *Phys. Rev. A* **57**, 4736-4746 (1998).
[9] J. J. Bollinger, W. M. Itano, D. J. Wineland & D. J. Heinzen, *Phys. Rev. A* **54**, R4649-R4652 (1996).
[10] A. Boto, et al. *Phys. Rev. Lett.* **85**, 2733-2736 (2000).
[11] M. D'Angelo, M. V. Chekhova & Y. Shih, *Phys. Rev. Lett.* **87**, 013602 (2001).
[12] E. J. S. Fonseca, Z. Paulini, P. Nussenzveig, C. H. Monken & S. Pádua, *Phys. Rev. A* **63**, 043819 (2001).
[13] M. W. Mitchell, J. S. Lundeen & A. M. Steinberg, *Nature* **429**, 161-164 (2004).
[14] P. Walther, J.-W. Pan, M. Aspelmeyer, R. Ursin, S. Gasparoni & A. Zeilinger, *Nature*, **429**, 158-161 (2004).
[15] E. Knill, R. Laflamme & G. J. Milburn *Nature* **409**, 46-52 (2001).
[16] G. J. Pryde & A. G. White, *Phys. Rev. A* **68**, 052315 (2003).
[17] J. Fiurášek, *Phys. Rev. A* **65**, 053818 (2002).
[18] H. Lee, P. Kok, N. J. Cerf & J. P. Dowling, *Phys. Rev. A* **65**, 030101 (2002).
[19] X. Zou, K. Pahlke & W. Mathis, quant-ph/0110149 (2001).
[20] P. G. Kwiat, W. A. Vareka, C. K. Hong, H. Nathel & R. Y. Chiao, *Phys. Rev. A* **41**, 2910-2913 (1990).
[21] J. G. Rarity, et al., *Phys. Rev. Lett.* **65**, 1348-1351 (1990).
[22] Z. Y. Ou, X. Y. Zou, L. J. Wang & L. Mandel, *Phys. Rev. A* **42**, 2957-2965 (1990).
[23] K. Edamatsu, R. Shimizu & T. Itoh, *Phys. Rev. Lett.* **89**, 213601 (2002).
[24] S. Takeuchi, J. Kim, Y. Yamamoto, and H. Hogue, *Appl. Phys. Lett.* **74**, 1063-1065, (1999).
[25] M. Reck, A. Zeilinger, H. J. Bernstein & P. Bertani, *Phys. Rev. Lett.* **73**, 58-61 (1994).
[26] Y. Aharonov, P. G. Bergmann & J. L. Lebowitz, *Phys. Rev.* **134**, B1410-B1416 (1964).
[27] D. T. Pegg, S. M. Barnett & J. Jeffers, *J. Mod. Optics* **49**, 913-924 (2002).
[28] K. L. Pegg, quant-ph/0508088 (2005).
[29] K. L. Pegg & D. T. Pegg, *Journal of Modern Optics* **51**, 1613 (2004).
[30] Z. Zhao, Y.-A. Chen, A.-N. Zhang, T. Yang, H. J. Briegel & J.-W. Pan, *Nature* **430**, 54-58 (2004).